JOURNAL OF PROPULSION AND POWER
Vol. 10, No. 2, March–April 1994

Axial Thrust Behavior in LOX-Pump of Rocket Engine

Junichi Kurokawa*
Yokohama National University, 156 Tokiwadai, Hodogaya-ku, Yokohama 240, Japan
and
Kenjiro Kamijo† and Takashi Shimura‡
National Aerospace Laboratory, 1, Kimisen, Koganezawa, Kakuta 981-15, Japan

The LOX pump of the first stage of the H-II rocket, the next generation of large launch vehicle in Japan, has shown fairly good axial thrust performance. However, the behavior of the axial thrust is not well known because of the complicated mechanism of the thrust-balancing device. In order to elucidate the flow characteristics of the complicated thrust balancing device and to improve it, the internal flow in the device was fully analyzed by developing a method of boundary value determination at each element composing the device. The analysis developed here was confirmed to give satisfactory results by comparison with actual measurements. Using the present analysis, the axial thrust behavior of the LOX pump was revealed for various combinations of balancing piston, balancing holes, swirl breaker, etc.

Nomenclature

AM	=	angular momentum of leakage flow
b	=	radial gap width of annular flow
C_q	=	leakage parameter, $(q/2\pi r_2^3\omega)Re^{1/5}$
K	=	tangential velocity ratio of core fluid, $v_\theta/r\omega$
M	=	friction moment of the wall
n	=	number of balancing holes, fastening bolts, or grooves of a swirl breaker
p, P	=	pressure and nondimensional pressure, respectively, $2p/\rho u_2^2$
q, Q	=	leakage flow rate and pump discharge, respectively
Re	=	Reynolds number, r_2u_2/ν
r, r_2	=	radius and main impeller radius, respectively
s	=	axial gap width of disk flow
u_2	=	main impeller tip speed
v	=	absolute velocity
z	=	axial distance from the wall
ζ_P	=	contraction coefficient of balancing piston A
λ	=	friction coefficient of annular gap
ν, ρ	=	kinematic viscosity and density of fluid, respectively
τ	=	wall shearing stress
ϕ	=	discharge coefficient of main impeller
ψ	=	pressure head coefficient of pump
ω	=	angular velocity of shaft

Subscripts

B, P, S	=	at balancing hole, balancing piston, and groove of a swirl breaker, respectively
I, O	=	at the inlet and the outlet of the control volume through which leakage flows
R, S, C	=	at the rotating, stationary, and cylindrical walls, respectively
r, θ, z	=	radial, tangential, and axial components, respectively
0	=	at the design point of the main pump

Presented as Paper 91-2410 at the AIAA/SAE/ASME/ASEE 27th Joint Propulsion Conference, Sacramento, CA, June 24–26, 1991; received July 8, 1991; revision received June 22, 1993; accepted for publication Aug. 3, 1993.

*Professor, Faculty of Engineering, Department of Mechanical Engineering and Materials Science.
†Head of Rocket Fluid System Section. Member AIAA.
‡Senior Researcher of Rocket Fluid System. Member AIAA.

I. Introduction

IT is obvious that the reliability and safety of pumps transferring hazardous liquids, such as LOX, LH_2, LPG, or LNG, greatly depend upon axial thrust balance, and that the adoption of a thrust balancing device is unavoidable. In such devices strong stiffness is required not only against static balance, but against dynamic balance. Thus, a complicated sealing system must also be adopted to prevent the leakage of hazardous liquids, and the thrust balancing device becomes very complex.

A LOX pump with a rotational speed of 20,000 rpm which will be used in the first stage of the next generation launch vehicle, the H-II rocket, in Japan, has shown fairly good thrust balance.[1,2] This pump has a unique thrust balancing device and two types of sealing systems, but the behavior of the axial thrust and the flow characteristics of the device are not yet well known.

In order to determine overall behavior of axial thrust in such a complicated device, the flow in each element composing the device must be carefully analyzed and combined one-by-one using the boundary values. However, it is still difficult to accurately determine the boundary values in a real machine because there are many types of boundary configurations, the flow behaviors of which are not yet well known, such as balancing piston, balancing hole, swirl breaker, etc. Thus, overall thrust behavior in such a complicated thrust-balancing device has not yet been reported.

One of the present authors has been studying the axial thrust of radial flow turbomachinery of simple configuration, and has found that the accuracy of the thrust calculation is mainly dependent upon the leakage flow rate and the boundary values of the pressure and the flow velocity.[3–5] Among the boundary values, the most important are those at the impeller outlet, a prediction method of which has also been developed by one of the present authors.[6,7]

The purpose of the present study is to develop a method of predicting the axial thrust of multistage pumps with complicated balancing devices, and to reveal the thrust behavior of the LOX pump developed in Japan.

II. Theoretical Analysis

Axial thrust is caused by pressure acting on the rotating parts of a machine. Axial thrust analysis therefore consists of analysis of flow in the gap between rotating and stationary walls and determination of boundary values. Generally, gap flow is of two types. One is the axial gap flow between a

rotating disk and a stator such as that at the back of an impeller shroud, and the other is the annular gap flow such as that in an annular seal. In the former, centrifugal force is dominant, while in the latter, wall shearing stress is dominant.

Gap flow analysis requires precise determination of the boundary values of flow velocity and pressure at the inlet and the outlet of all the gaps, that is at the entrance and the exit of an impeller as well as at an inducer and guide vanes. The boundary values at an impeller outlet are predicted by one of the present authors' methods,[6,7] and those at the outlet of an inducer and guide vanes are predicted by using an ordinal two-dimensional cascade theory.

A. Analysis of Axial Gap Flow

As shown in Fig. 1, the flow in the axial gap between a rotating disk and a stationary wall consists of the boundary-layer flows along both disk walls, and the core flow in which the tangential velocity v_θ is expressed as $Kr\omega$ and no radial flow is induced. The flow characteristics are determined from the equations of momentum, angular momentum, and continuity represented by

$$\frac{\partial}{\partial r}\left(r\int_0^s v_r^2\,dz\right) - \int_0^s v_\theta^2\,dz = -\left(\frac{rs}{\rho}\right)\left(\frac{dp}{dr}\right) - \frac{r(\tau_{Rr} + \tau_{Sr})}{\rho} \tag{1}$$

$$\frac{\partial}{\partial r}\left(r^2\int_0^s v_r v_\theta\,dz\right) = -\left(\frac{r^2}{\rho}\right)(\tau_{R\theta} + \tau_{S\theta}) \tag{2}$$

$$2\pi r\int_0^s v_r\,dz = q \tag{3}$$

Assuming the one-seventh power law for the velocity distribution in the boundary layers and shearing stress of Blasius type for hydraulically smooth walls, the above equations are transformed into two ordinary differential equations with regard to the core velocity ratio K, and the nondimensional pressure P as a function of the radius ratio r/r_2. The governing equations are also obtained for the case of a rough wall by assuming the logarithmic velocity profile,[4] and for a very narrow gap so that the boundary layers on both walls interfere with each other.[5]

Analysis of the results reveals that the parameters having the greatest influence upon the characteristics of axial gap flow are C_q, the tangential velocity ratio K_I of the leakage before entering the gap, the axial space ratio s/r_2, the relative surface roughness, and Re.

Analysis of the axial gap flow requires the accurate value of C_q, which is determined based on the pressure drop at balancing holes or annular seals, but the pressure drop also varies with the leakage. A trial-and-error method is therefore needed to determine a higher approximation of leakage by assuming the first one.

B. Analysis of Annular Gap Flow

λ is usually determined under the assumption that the gap fluid rotates at half the velocity of the rotating wall.[8] However, the calculated results have revealed that the prerotation of leakage $K_I r\omega$, entering an annular gap has remarkable influence on the fluid rotational velocity $Kr\omega$ in the gap. The momentum balance and the angular momentum balance in an annular gap are expressed as follows using the pressure difference Δp:

$$AM_O - AM_I = 2\pi l[r^2\tau_{R\theta} - (r + b)^2\tau_{S\theta}] \tag{4}$$

$$\pi(2r + b)b\Delta p = 2\pi l[r\tau_{Rz} + (r + b)\tau_{Sz}] \tag{5}$$

Assuming the one-seventh power law of velocity and Blasius-type shearing stress, and considering the hydraulic losses at the inlet and outlet of the gap in Eq. (5), the above equations become

$$0.0267\{(1 - K)[(1 - K)^2 + Y^2]^{3/8} - K(K^2 + Y^2)^{3/8}\}/Re_z^{0.24} = (q/2\pi r^2 l\omega)[1 + 16(K - K_I)]/18 \tag{6}$$

$$\Delta P = (\lambda l/2b + 1.5)(v_z/u_2)^2$$

$$\lambda = 0.130\{[1 + (K^2/Y^2)]^{3/8} + [1 + (1 - K)^2/Y^2]^{3/8}\}/Re_z^{0.24} \tag{7}$$

where $Re_\omega = rb\omega/\nu$, $Re_z = v_z b/\nu$, $Y = (8/7)(Re_z/Re_\omega)$. If $K = 0.5$, the above λ-formula (7) agrees with the conventional one.[8]

C. Determination of Boundary Values of Velocity and Pressure

The boundary values of velocity can be determined by considering angular momentum balance at every boundary. The determination of boundary pressure requires hydraulic loss analysis, however, it is still difficult to estimate losses in several components of a thrust-balancing device, such as a balancing hole, a balancing chamber, a swirl breaker, etc. Simplified flow models in the components and hydraulic loss formulas are presented in this chapter.

1. *Velocities at Boundaries*

The boundary value of K is determined based on the angular momentum balance in the control volume assumed at the boundary of the flowfield. There are various types of boundary conditions and a typical case is illustrated in Fig. 2. The leakage from an annular gap enters the control volume ABCDE surrounded by the rotating wall Ⓡ and the stationary wall Ⓢ with an angular momentum of AM_I and exits with

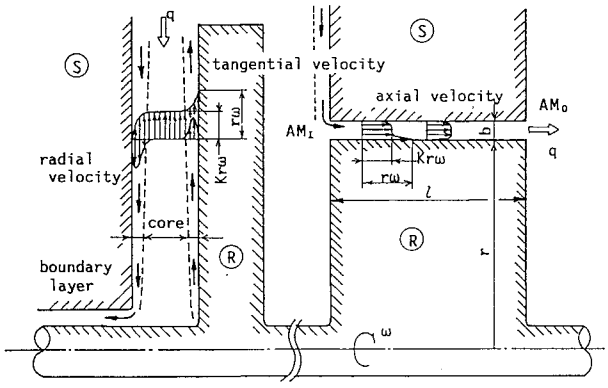

Fig. 1 Flow in axial gap and annual gap and symbols.

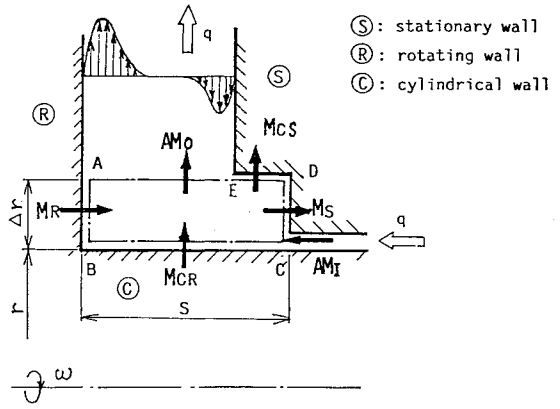

Fig. 2 Angular momentum balance at the boundary of a gap.

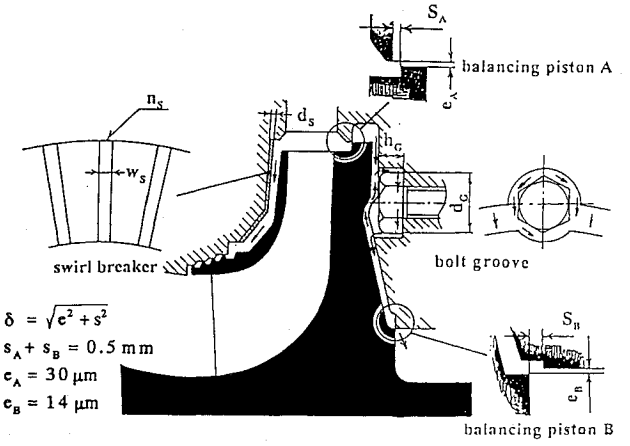

Fig. 3 Balancing pistons *A* and *B*, swirl breaker and bolt groove.

AM_O per unit time; the friction torque M_R and M_{CR} are supplied by the rotating wall; and the friction torque M_S and M_{CS} are consumed by the stationary wall. Thus, the boundary condition is

$$AM_O - AM_I = M_R - M_S + M_{CR} - M_{CS} \quad (8)$$

The right side of Eq. (8) is calculated by assuming the one-seventh power law for boundary-layer velocity distribution and the Blasius type shearing stress. The outlet angular momentum AM_O is calculated considering the type of leakage exit, such as into an axial gap, into a stationary annular gap, or into a rotating annular gap. The inlet angular momentum AM_I is also calculated by considering the type of leakage entrance and prerotation.[3,5] The boundary equation is thus obtained, and the boundary values of K are determined for all sections where the dimensions and the configurations of the axial gap change.

2. Balancing Piston, Balancing Holes, and Labyrinth Seals

The balancing piston shown in Fig. 3 is adopted for the LOX pump. As the gap δ is very narrow, it can well be assumed that the velocity head through this gap is not recovered. Thus, the pressure loss ΔP of the balancing piston is expressed when a contraction coefficient C_c of a pipe orifice is introduced as

$$\Delta P_P = \zeta_P(q_P/2\pi r_P \delta u_2 C_c)^2, \quad C_c = 0.600, \quad \zeta_P = 1.00 \quad (9)$$

The flow in a balancing hole is usually approximated to the rotating pipe flow. However, the inlet flow has large relative rotation, and the pipe length is very short. Accordingly, the flow rate coefficient must be much different from that of a usual pipe, and one of the present authors has determined the following empirical formula.[9]

$$q_B = \kappa n_B(\pi d_B^2/4)\sqrt{2\Delta p_B/\rho}, \qquad \kappa = 0.00155 Re_B^{0.568} \quad (10)$$

For $Re > 9 \times 10^4$, the value of $\kappa = 1.0$ is used.

As for the flow in labyrinth seals, many studies have been made of the parallel-type seal, but the loss in the step-type seal shown in Fig. 3 is not yet clear.[10] The parallel-type seal utilizes contraction effect, and the step-type seal uses both contraction effect and centrifugal force effect. For the sake of simplicity, the head loss in the parallel type is herein considered to consist of sudden expansion and friction, and for the step-type seal the pressure drop due to centrifugal force is also added as follows:

parallel-type

$$\Delta P = (1.5 + \lambda l/2b)(v_z/u_2)^2 \quad (11)$$

step-type

$$\Delta P = (1.5 + \lambda l/2b)(v_z/u_2)^2 + \Sigma K^2(r_o^2 - r_i^2)/r_2^2 \quad (12)$$

3. Swirl Breaker

An effective method of reducing total axial thrust is to increase an axial force toward the reverse direction, with a swirl breaker such as shown in Fig. 3 being used. Several radial grooves are made on the casing wall, and the fluid rotation is considerably reduced by these grooves, of which mechanism is not yet clear. The radial inward leakage loses its tangential velocity when it enters a radial groove at the outer radius, and the flow can be analyzed by considering the additional angular momentum loss[11] in Eq. (2). As the flow in a groove is induced by the radial pressure gradient dp/dr $(=\rho K^2 r\omega^2)$, the angular momentum loss AM_S, and the flow rate q_S in the groove can be estimated by the following formula:

$$AM_S = \rho q_S K r^2 \omega, \qquad q_S = n_S d_S w_S K \omega \sqrt{8 r_S r/\lambda} \quad (13)$$

where r_S, n_S, d_S, and w_S are the hydraulic radius, the number, the depth, and the width of the groove, respectively. The above AM_S is subtracted from the right side of Eq. (2), and q_S is subtracted from the right side of Eq. (3).

III. Dimensions of LOX-Pump Tested and Input Data

A schema of the whole LOX pump of the H-II rocket is shown in Fig. 4. A portion of the LOX discharged from the main impeller is again pumped by a smaller impeller (preburner impeller) into the preburner, where it is mixed with LH_2 and is combusted. The mixed gas drives the turbine and then enters the main combustion chamber. The LOX pump tested consists of the main and the preburner impellers arranged back-to-back; two types of seals are used to isolate the LOX and the mixed gas. The inducer and the guide vanes are installed at the main impeller entrance. A slinger with radial vanes is also installed to reduce the pressure of the leakage flow.

The thrust balancing device consists of variable orifices, A and B shown in Fig. 4, which adjust the gap at the back of the main impeller automatically. If the axial thrust toward suction becomes larger, the gap at A becomes smaller, which causes a decrease in pressure and results in the axial thrust toward suction becoming smaller again. On the contrary, if the thrust force toward turbine becomes larger, orifice B comes into play.

As the gaps at orifice A and orifice B are very small as shown in Fig. 3, the deformation due to centrifugal force and inner pressure must be taken into account in addition to consideration of the assembly tolerance. Several gaps around the main impeller were measured by the calibrated gap sensor of an eddy-current type. The measured gap at the assembly was $e_A = 38$ μm, but became 30 μm during operation because of an elongation of 30 μm of the inner wall and 22 μm of the outer wall. The gap of orifice B was $e_B = 14$ μm during pump operation.

The measurements were performed using LOX at -181°C and LH_2 at -193.5°C. The property of the liquid used is shown in Table 1. The flow rates in the main pump and in the preburner pump were measured by calibrated turbine meters.

Table 1 Physical properties of LOX (−181°C) and LH_2 (−193.5°C) at atmospheric pressure

	p, MPa	Temperature, K	ρ, kg/m³	μ, N·s/m²
LN_2	0.1013	77.4	808	1.63×10^{-4}
LOX	0.1013	90.2	1140	1.96×10^{-4}

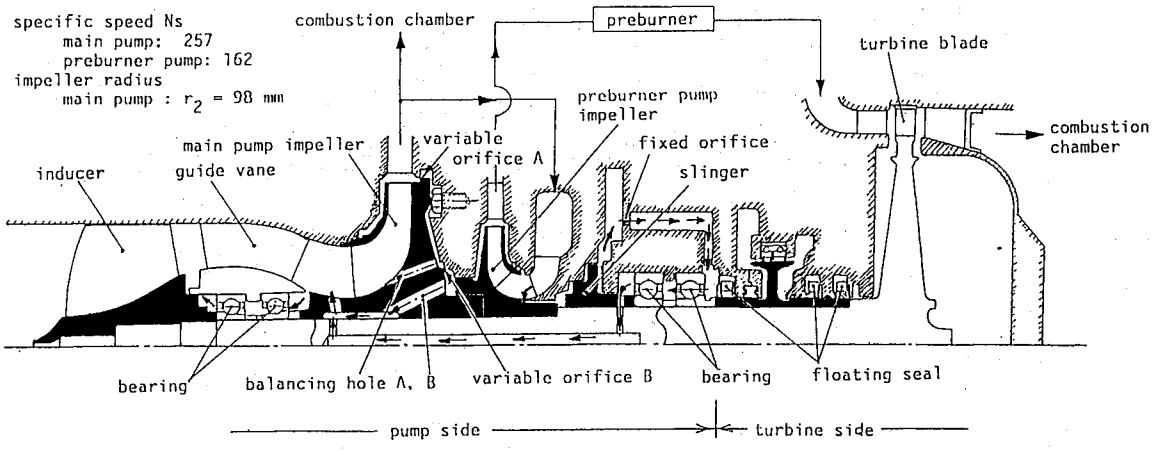

Fig. 4 Schema of the whole LOX turbopump used in the *H*-II rocket.

The pump tested has six leakage passes. They are two cooling and lubrication passes of the front and rear bearings, two leakage passes through the front shroud gaps of the main and the preburner impellers into the suction side, and two leakage passes through the back shroud gaps of both impellers into the main impeller eye through the balancing holes *A* and *B*. The rear bearing cooling pass branches into two passes, joins into one, and flows through the center axis hole.

Calculations are performed in each pass by assuming the first approximation of C_q, then the pressure distribution is calculated. The leakage of higher accuracy is asymptotically determined.

IV. Comparison of Theory with Measurements

The theoretical analysis is performed for the following three cases in which full measurements of pressure and axial thrust were performed with high reliability.

Test no. 1 (LN2 test): 20,600 rpm, 95% of the design flow rate, with balancing hole *B* and two fixed orifices.

Test no. 2 (LN2 test): 20,160 rpm, 97% of the design flow rate, with balancing holes *A* and *B* and one fixed orifice.

Test no. 3 (LOX test): 20,100 rpm, 102% of the design flow rate, with balancing holes *A* and *B* and one fixed orifice.

The predicted head curve of the main impeller is compared with the measurements in Fig. 5, which includes the predicted head at the inducer outlet and at the impeller inlet. They agree very well and the inducer head amounts to about 23% of the main impeller head at the design flow rate. The behavior of axial thrust shown below is analyzed based on the above predicted values of pressure and velocity as the boundary values.

A. Some Problems Arising from Analyzed Results

The predicted pressure distribution at every rotating part showed fairly good agreement with the measurements except for one part, i.e., the rear shroud gap of the main impeller. Thorough examination of the impeller and casing revealed that the disagreement was due to the annular groove with a row of fastening bolts machined on the casing wall as shown in Figs. 3 and 4.

In this case the flow around the groove can be modeled as a rotational flow with a row of circular cylinders surrounded by two annular walls. Here, K can also be determined from Eq. (2) by subtracting the following angular momentum loss due to the drag of the cylinder row from the right side[11]

$$\rho r d_G n_G C_D \int_o^{h_G} (v_r^2 + v_\theta^2)^{0.5} v_\theta \frac{dz}{2}, \qquad C_D = 2.05 \quad (14)$$

where the symbols used are those shown in Fig. 3, and C_D is a drag coefficient of circular cylinder.[12]

The calculated results reveal that the fluid rotates at less than $0.1r\omega$ at the groove, and that flow with small angular momentum comes into the inner radius, which results in the fluid rotating very slowly, and consequently, the pressure being almost uniform in the inner radius of the groove. This fact suggests that the existence of such resistance makes axial thrust considerably larger, not only in the thrust balancing device but also in the usual rotational flowfield.

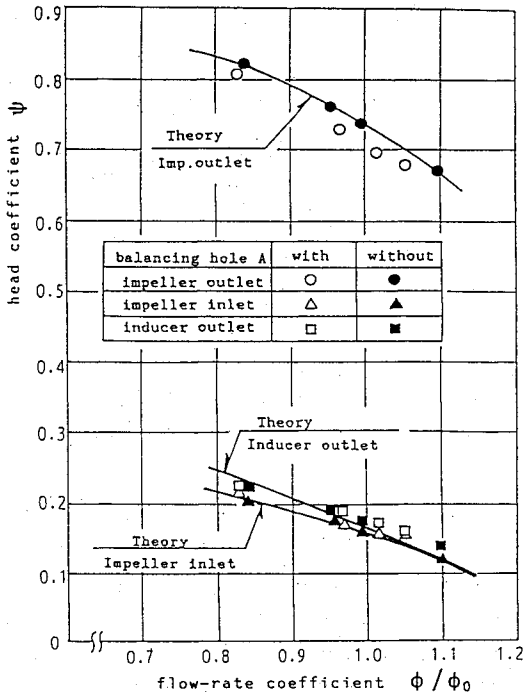

Fig. 5 Head curves of main impeller and inducer.

B. Axial Thrust Behavior

The axial thrust on the pump side varies rapidly with gap s_A at variable orifice *A*. Accordingly, calculations are performed to demonstrate the effect of variations in this gap.

The axial thrust and the leakage characteristics are shown in Fig. 6, in which thrust toward the suction side is assumed to be positive. It is seen that the axial thrust decreases considerably with a decrease in gap s_A. The main difference between test no. 1 and no. 2 (and no. 3, i.e., LOX test) is that balancing hole *A* is installed in the latter; the comparison of the thrust curves of test nos. 1 and 2 (and 3) reveals that the installation of balancing hole *A* decreases the total axial thrust considerably. It is also observed from Fig. 6 that the leakage is not increased by installation of balancing hole *A* when s_A is less than 0.15 mm, while for the wider range of s_A the leakage becomes much larger. The above described characteristics are typical of this type of balancing piston.

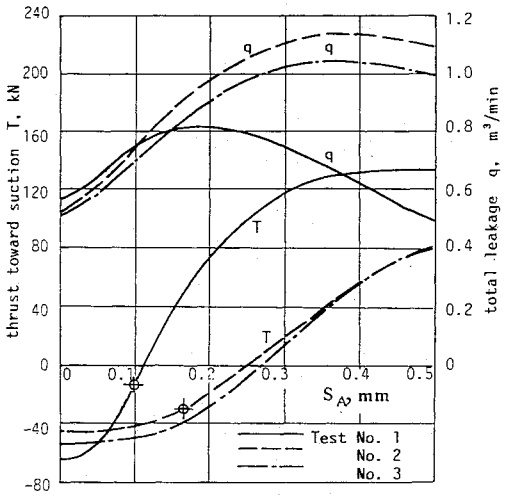

Fig. 6 Total axial thrust and leakage vs axial gap at balancing piston A.

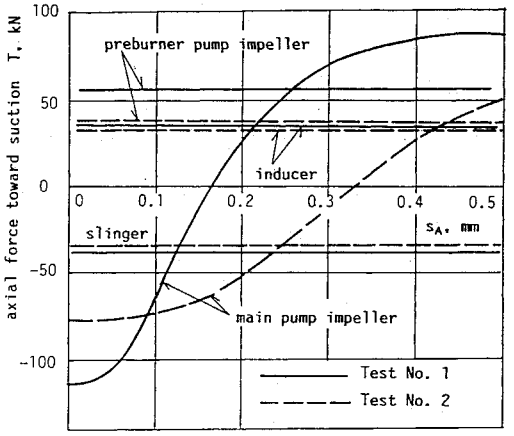

Fig. 7 Each component of axial thrust vs axial gap s_A.

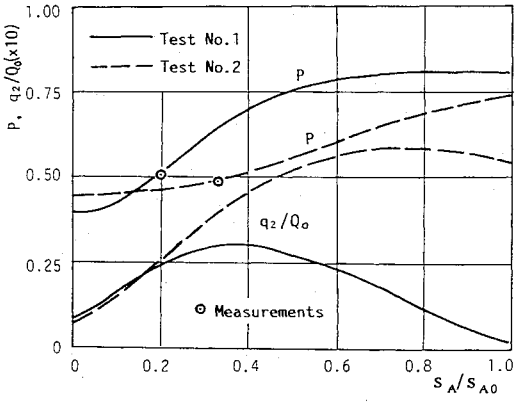

Fig. 8 Pressure and leakage variation at the back of the main impeller (s_{A0} = 0.5 mm).

The stability of the thrust balancing device can be estimated by the gradient dT/ds_A of the thrust curve. When there is no balancing hole A (test no. 1), about 8 tons are needed to move the axis by 0.1 mm near the point of $T = 0$. This indicates that this device has strong stiffness and is stable against thrust variation. The installation of balancing hole A (test no. 2), however, results in a very gentle thrust curve.

To determine operating gap s_A of the balancing device theoretically, the value of the thrust force on the turbine rotor is needed. This value changes rapidly depending upon the turbine operating conditions, though it is much smaller than that on the pump impeller. As the thrust force on the turbine side is not known, balancing gap s_A is determined so that the

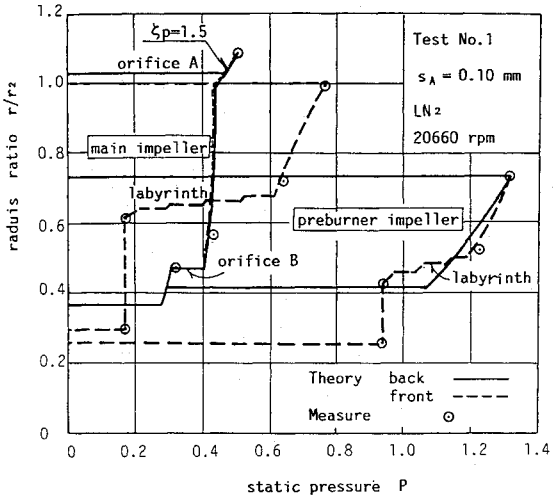

Fig. 9 Pressure distribution around the main and the preburner impellers at test no. 1 (no balancing hole A).

predicted pressure at the balancing chamber of variable orifice A is equal to the measured pressure. Balancing gap s_A so determined is indicated by ⊕ in Fig. 6, and is 0.10 mm for test no. 1 and 0.17 mm for test no. 2. It is thus concluded that the operating gap becomes 1.7 times wider due to the installation of balancing hole A, which promotes pump reliability.

The axial thrust is composed of axial forces on every rotating part; the variation of each axial force is shown in Fig. 7. The predicted axial forces on the inducer and the slinger are seen to be nearly equal in magnitude and reverse in direction, so that they cancel out each other. Accordingly, the total axial thrust behavior is determined as the balance between the axial force on the main impeller and on the preburner impeller. For variations of s_A, the axial force on main impeller varies rapidly, but that on the preburner impeller varies slightly. This is because the change of leakage with gap s_A is large in the main impeller, but small in the preburner impeller. It is interesting that the direction of the axial force of the preburner impeller is reverse to that of ordinary pumps. This is because the leakage in the rear shroud gap is 43% larger than that in the front shroud gap.

To clarify the thrust variation with gap s_A, the variation of P in the balancing chamber A is shown in Fig. 8 together with leakage q_2 at the back of the main impeller. The pressure curve is seen to be very similar to that of the total thrust in Fig. 6 and the axial force on main impeller in Fig. 7. Furthermore, the leakage curve is also very similar to that of the total leakage in Fig. 6. This reveals that the variations of total thrust and leakage are mainly caused by balancing piston A.

C. Comparison of Pressure Distribution

The calculated pressure distributions around the main and the preburner impellers are compared with the measured distributions in Fig. 9 in which the solid lines show the rear shroud side and the dotted lines the front shroud side. The present theory is seen to give satisfactory pressure distributions, including the boundary values at the impeller outlet. The pressure distribution at the back of the main impeller rear shroud is seen to be very uniform in spite of the large leakage, which is due to the effect of the bolt groove as mentioned in Sec. IV.A. This reveals that the annular groove with obstacles on the casing wall is very effective in reducing the axial thrust.

Further calculation is performed to examine the resistance of the variable orifice by changing the orifice loss coefficient ζ_p from 1.0 to 1.5. The calculated result is shown by the chain-dotted line in Fig. 9. It is recognized that the pressure hardly changes in spite of considerable change in the loss coefficient.

This is because the increase in orifice resistance results in a decrease in leakage to 83%. As a result, the pressure loss in the orifice A hardly changes. Such a case corresponds to gap blockage due to obstacles or to gap damage. The present self-balancing device is proved to have strong stiffness and high reliability.

Calculation was also performed for the case of test no. 2 (with balancing hole A), and comparison between test no. 1 and test no. 2 revealed that the pressure in the rear gap of the main impeller decreases about 5% due to balancing hole A. That is to say, the effect of balancing hole A is only a 5% decrease in pressure, but it results in a large decrease of axial thrust as shown in Fig. 7. This causes the variable orifice gap to become wider on the safe side.

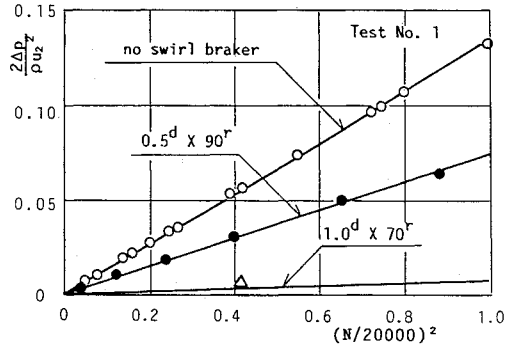

Fig. 10 Pressure drop at the main impeller front shroud and the effect of swirl breaker.

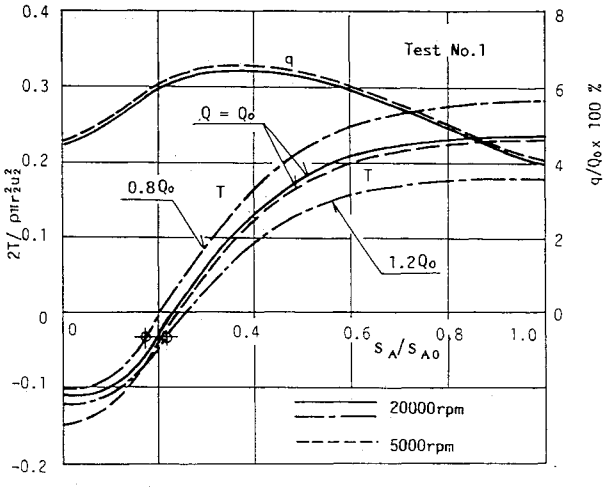

Fig. 11 Thrust performance at the off-design operation and the Reynolds number effect.

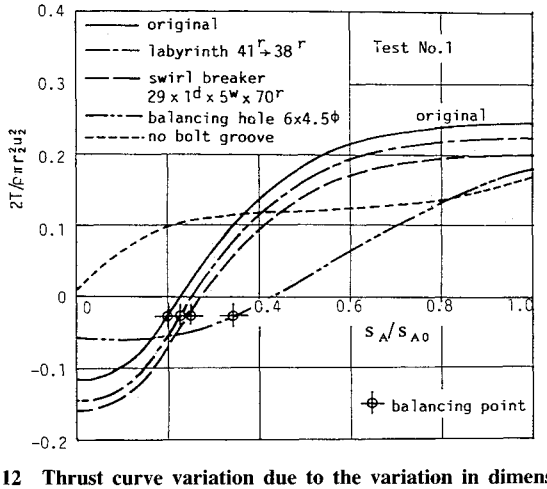

Fig. 12 Thrust curve variation due to the variation in dimensions (test no. 1).

D. Effects of Swirl Breaker

A swirl breaker installed on the front casing wall of the main impeller decreases the radial pressure drop and increases the axial force toward discharge, which results in a large decrease in total axial thrust. The calculated pressure drop from $r/r_2 = 1.0$ to 0.71 is compared with the measured drops in Fig. 10 for two types of swirl breakers. It is recognized that the radial grooves with a depth of only 0.5 mm decrease the pressure drop considerably, while those with a depth of 1 mm result in almost uniform radial pressure distribution. The present analysis shown by the solid lines gives an accurate estimation of the effects of a swirl breaker. The effect of a swirl breaker is mainly due to the angular momentum loss of the fluid entering the radial grooves, and its effect is mainly dependent on the total sectional area of the grooves. The angular momentum loss is especially large at the outer radii because the rotating velocity there is very large. Accordingly, short grooves sufficiently reduce total axial thrust, if they are installed at the outer radii.

E. Axial Thrust Performance at Off-Design Operation

The above-described thrust performances are near the designed point of pump operation. In the off-design operation, the axial thrust curve varies depending on the pumping head as shown in Fig. 11 for two cases of flow rates of $1.2Q_0$ and $0.8Q_0$. s_A becomes slightly larger at higher flow rates, and smaller at lower flow rates. In Fig. 11, the thrust curves at different rotational speed are also shown, and it is recognized that the nondimensional quantities of axial thrust and leakage become slightly larger with the Reynolds number, and that s_A changes little for the change of the pump rotational speed.

F. Some Improvement in the Thrust Balancing Device

As the present analysis is confirmed to give satisfactory results, further calculations are performed to improve the thrust balancing device. Several variations of the main parameters influencing total axial thrust are tested, such as changing the diameter of balancing hole A and that of the labyrinth seal at the back of the preburner impeller, installing a swirl breaker on the front casing wall, or removing the bolt groove at the back of the main impeller. The calculated results are shown in Fig. 12 for test no. 1.

The calculated results show that s_A can be made a little wider by reducing the labyrinth diameter at the back of the preburner impeller, or by installing a swirl breaker on the front casing wall without losing the stiffness of the balancing device. The installation of A makes the operating gap much wider, though the thrust curve becomes very gentle and the stiffness of the balancing device greatly decreases. In the transient operation, A has an important role of attaining a rapid decrease of pressure at the back of the main impeller.

It should be noted that the removal of the bolt groove at the back of the main impeller makes the thrust curve very unstable, and that s_A becomes negative. This implies that the bolt groove has an important role of balancing the axial thrust of this pump, and that it is difficult to ensure a sufficient operating gap without the bolt groove, even if several improvements are attained.

V. Conclusions

A method of theoretical analysis for predicting axial thrust and leakage of multistage centrifugal pumps with complex thrust balancing devices has been established. Using this method, the thrust and leakage performances of the LOX turbopump of the H-II rocket can be elucidated; results are summarized as follows:

1) Comparison of the present predictions with the measurements revealed that the angular momentum balance pre-

sented here yields satisfactory results including the boundary values and also the accurate prediction of axial thrust behavior. It is here very important to correctly predict the effects of annular and axial grooves installed in the casing wall.

2) The axial thrust of the LOX pump greatly varies with the gap of the balancing piston, and the present balancing device has significant stiffness against thrust variation, although the operating gap is as narrow as 0.10 mm. When balancing hole A is installed, the operating gap increases 1.7 times and the reliability of the device increases, though the stiffness greatly decreases.

3) The operating gap of the balancing piston varies little with the variations of impeller rotational speed. It decreased a little in the smaller pump discharge range and increases a little in the larger discharge range. By the adoption of balancing holes the leakage changes little at the operating gap.

4) The balancing piston adopted has high reliability against gap blockage or damage, and the operating gap hardly changes for large variation of leakage, as the pressure changes little.

5) The existence of obstacles, such as a row of bolts in an annular groove, decreases the fluid peripheral velocity substantially and makes the radial pressure distribution nearly uniform, thereby allowing a considerable axial force. However, if it were not for the annular grooves in the present device, it would be very difficult to ensure an operating gap of sufficient width.

6) The prediction of a swirl breaker is also presented. A swirl breaker is effective in increasing a negative axial thrust and an operating gap, but the effect is limited to some extent up to a zero pressure drop. The effect depends mainly upon the total sectional area of the grooves.

References

[1]Kamijo, K., and Hirata, K., "Performance of Small High Speed Cryogenic Pumps," *Journal of Fluid Engineering*, Vol. 107, June 1985, pp. 197–204.

[2]Kamijo, K., Yoshida, M., Watanabe, Y., Hashimoto, R., Ohta, T., and Warashina, S., "Development Status of LE-7 LOX Turbopump," *Proceedings of 16th International Symposium on Space Technology and Science* (Sapporo, Japan), I.S.T.S. Organizing Committee, 1988, pp. 281–288.

[3]Kurokawa, J., and Toyokura, T., "Study on Axial Thrust of Radial Flow Turbomachinery," *Proceedings of 2nd JSME Symposium on Fluid Machinery and Fluidics* (Tokyo), Japan Society for Mechanical Engineering, 1972, Vol. 1, pp. 31–40.

[4]Kurokawa, J., Toyokura, T., Shinjo, M., and Matsuo, K., "Roughness Effects on the Flow Along an Enclosed Rotating Disk," *Bulletin of the Japan Society of Mechanical Engineers*, Vol. 21, No. 162, 1978, pp. 1725–1732.

[5]Kurokawa, J., and Sakuma, M., "Flow in a Narrow Gap Along an Enclosed Rotating Disk with Through-Flow," *JSME International Jr., Ser. 2*, Vol. 31, No. 2, 1988, pp. 243–251.

[6]Kurokawa, J., and Jiang, J., "Performence Prediction of Centrifugal Impellers and Scale Effects," *Proceedings of International Symposium on Large Hydraulic Machinery and Associated Equipments* (Beijin), International Research Centre on Hydraulic Machinery, Vol. 1, 1989, pp. 56–67.

[7]Kurokawa, J., and Hode, S., "Prediction of Outlet Flow Characteristics of Centrifugal Impellers (1st Report)," *Bulletin of the Japan Society of Mechanical Engineers*, Vol. 28, No. 241, 1985, pp. 1423–1429.

[8]Yamada, Y., "Resistance of Flow through an Annulus with an Inner Rotating Cylinder," *Bulletin of the Japan Society of Mechanical Engineers*, Vol. 5, No. 18, 1962, pp. 302–310.

[9]Kurokawa, J., "Simple Formulae for Volumetric Efficiency and Mechanical Efficiency of Hydraulic Machinery," *Proceedings of 3rd Japan-China Conference on Fluid Machinery* (Osaka, Japan), Turbomachinery Society of Japan, Vol. 1, 1990, pp. 101–108.

[10]Eichler, O., and Wiedmann, M., "Untersuchung gestufter Spaltdichtungen für hydraulische Stroemungsmaschinen," VDI Berichte, Nr. 424, St. 53-62, 1981.

[11]Kurokawa, J., "A New Device to Control Axial Thrust of Radial Flow Turbomachinery," *Bulletin of the Japan Society of Mechanical Engineers*, Vol. 19, No. 128, 1976, pp. 110–117.

[12]Hoerner, S. F., "Fluid-Dynamic Drag," Hoerner, NJ, 1958, pp. 3–17.